

## Dielectric exchange-force effect on the rupture force of adsorbed bilayers of self-assembled surfactant films

O. Teschke, G. Ceotto, and E. F. de Souza

Citation: [Applied Physics Letters](#) **78**, 3064 (2001); doi: 10.1063/1.1358369

View online: <http://dx.doi.org/10.1063/1.1358369>

View Table of Contents: <http://scitation.aip.org/content/aip/journal/apl/78/20?ver=pdfcov>

Published by the [AIP Publishing](#)

---

### Articles you may be interested in

[On one-dimensional self-assembly of surfactant-coated nanoparticles](#)

*J. Chem. Phys.* **125**, 194717 (2006); 10.1063/1.2375091

[The influence of chain length and ripening time on the self-assembly of alkylamines on mica](#)

*J. Chem. Phys.* **125**, 044708 (2006); 10.1063/1.2221692

[Cosurfactant and cosolvent effects on surfactant self-assembly in supercritical carbon dioxide](#)

*J. Chem. Phys.* **122**, 094710 (2005); 10.1063/1.1855291

[Ge dots self-assembling: Surfactant mediated growth of Ge on SiGe \(118\) stress-induced kinetic instabilities](#)

*Appl. Phys. Lett.* **83**, 4833 (2003); 10.1063/1.1633012

[Morphological instabilities of the InAs/GaAs\(001\) interface and their effect on the self-assembling of InAs quantum-dot arrays](#)

*Appl. Phys. Lett.* **81**, 2270 (2002); 10.1063/1.1508416

---



**AIP** | Journal of  
Applied Physics

*Journal of Applied Physics* is pleased to  
announce **André Anders** as its new Editor-in-Chief

## Dielectric exchange-force effect on the rupture force of adsorbed bilayers of self-assembled surfactant films

O. Teschke<sup>a)</sup>

*Nano-Structure Laboratory, IFGW/UNICAMP, 13081-970, Campinas, SP, Brasil*

G. Ceotto

*Departamento de Física, Universidade Federal de Viçosa, 36571-000, Viçosa, MG, Brasil*

E. F. de Souza

*Instituto de Ciências Biológicas e Química, Pontifícia Universidade Católica de Campinas, 13020-904, Campinas, SP, Brasil*

(Received 6 December 2000; accepted for publication 29 January 2001)

We measured and formulated dielectric exchange forces between adsorbed layers of self-assembled surfactant films and atomic-force microscope tips in water. The dielectric exchange-force model is in agreement with the observation that the surfactant-layer rupture forces (tip-applied force necessary to obtain tip/substrate contact) are smaller in the thickest layers, where the compactness of the adsorbed film results in the smallest values of the dielectric permittivity. Within experimental accuracy, a dielectric permittivity value of  $\sim 4$  for bilayers and of  $\sim 36$  for monolayers is found. © 2001 American Institute of Physics. [DOI: 10.1063/1.1358369]

The structural and dynamical properties of adsorbed molecular thin films are of both fundamental and applied interest in diverse areas such as the statistical mechanics of complex fluids, thin-film boundary lubrication, and coatings, and have been the subject of recent experimental and theoretical investigations.<sup>1–3</sup> An intermolecular surfactant interaction in solution leads to a variety of self-assembled liquid-crystalline structures that have been well studied. At an interface, however, the normal self-assembly process is perturbed by competing surfactant–surface and solvent–surface interactions.

We explored the surfactant adsorbed structure by measuring the force acting on the tip when immersed in self-assemblies of cationic surfactant films at the interface between an aqueous solution and a substrate. For this purpose atomic-force microscope (AFM) topographic views and force curves were used to characterize structurally different adsorbed layers.

Surfactant adsorption was accomplished merely by introducing an aqueous solution of  $5 \times 10^{-5}$  M CTAB [cetyltrimethylammonium bromide,  $C_{16}H_{33}(CH_3)_3N^+Br^-$ ,  $cmc = 0.9$  mM] into the fluid cell and allowing the tip and freshly cleaved mica to stand in this solution before operation. CTAB was used as supplied, without further purification; solutions made of water (Milli-Q Plus quality, resistivity  $\sim 15$  M $\Omega$ /cm) were introduced into the cell after the substrate was mounted on the  $xyz$  translator of the AFM. All force curves and images were obtained in water or surfactant solutions by a commercial AFM TopoMetrix TMX2000 at room temperature, 25 °C, above the Krafft temperature of the surfactant. Both unmodified silicon nitride ( $Si_3N_4$ ) tips ( $\epsilon_T = 7.4$ ) and tips etched in 50% w/w HF solutions for 10 min before operation were used. The surface of a  $Si_3N_4$  tip in aqueous solution is composed of amphoteric silanol and ba-

silylamine [secondary and/or primary amines, though the latter is rapidly hydrolyzed] surface groups,<sup>4</sup> at  $pH \sim 6$ , with no added electrolyte the  $Si_3N_4$  surface is either *zwitterionic* (zero net charge) or slightly negatively charged;<sup>5</sup> consequently, we assumed that the surface charge density in the tip  $\sigma_{Tip} \ll \sigma_{Mica}$ . Platinum-coated tips ( $\epsilon_T \approx \infty$ ) were also used. When the mica basal plane is placed within water the mechanism for the formation of the double layer is assumed to be the dissolution of  $K^+$  ions as well as ion exchanging of  $K^+$  by  $H^+$  or  $H_3O^+$  ions. When CTAB is added to water  $K^+$  ions are also substituted by  $C_{16}H_{33}(CH_3)_3N^+$ .

AFM images clearly show that upon extended exposure that the CTAB molecules aggregate to form islands on the mica surface.<sup>6</sup> Figure 1 shows different aggregate sizes adsorbed at the interface. In order to determine the film thickness, force curves at the islands (region I) and outside (region II) were measured. In these curves the vertical axis represents the force acting between the tip and the sample

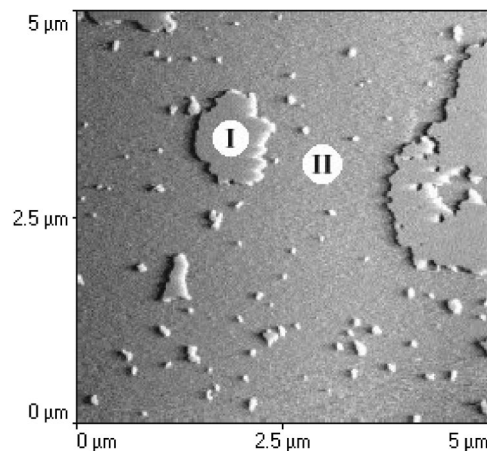


FIG. 1. AFM image of a CTAB adsorbed layer on mica in  $5 \times 10^{-5}$  M CTAB solutions. The islands (patches, I) indicate higher structures than the background (II).

<sup>a)</sup>Electronic mail: oteschke@ifi.unicamp.br

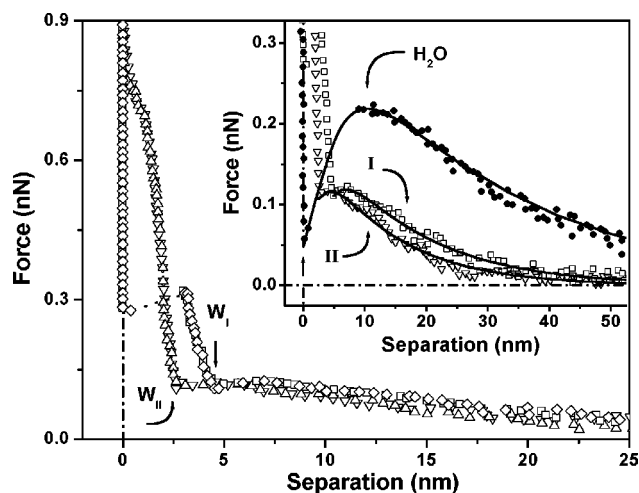


FIG. 2. Force vs absolute distance (separation) curves for CTAB adsorbed layers on mica in  $5 \times 10^{-5}$  M CTAB solutions for the regions shown in Fig. 1 [curve I ( $\square$  and  $\diamond$ , for  $v=1$  and  $5 \mu\text{m/s}$ , respectively) and curve II ( $\triangle$  and  $\nabla$ , for  $v=0.1$  and  $1 \mu\text{m/s}$ , respectively)]. The inset shows the fitted values calculated by Eq. (1) to the experimental points. All curves show an exponential profile as a function of separation  $H$  for  $H \gg 1$  nm.

surface. The horizontal axis represents the distance the sample is moved up and down by the  $xyz$  translator. In this curve repulsive and attractive forces act between tip and sample before contact. Hence, when the sample approaches the tip, the cantilever bends upwards. At a certain point the tip is attracted to the surface. Finally, moving the sample still further causes a deflection of the cantilever by the same amount the sample is moved. The approaching force curve is a plot of the change in cantilever deflection ( $\Delta Y$ ) versus sample displacement ( $\Delta X$ ). On a hard nondeformable surface,  $\Delta Y$  is proportional to  $\Delta X$  while the tip and the sample are in contact. Rather than using sample position ( $X$ ), it is more useful to use an absolute distance ( $H$ ) that is relative to the separation between the tip and the sample surface. The correction to produce a force-separation curve uses the relationship  $H = \Delta X + \Delta Y$ .<sup>7</sup> The following force curves show the force versus separation (absolute distance) plots. The two different regions show distinct force versus separation curves [curve I ( $\square$  and  $\diamond$  for  $v=0.1$  and  $1 \mu\text{m/s}$ , respectively) and curve II ( $\triangle$  and  $\nabla$  for  $v=1$  and  $5 \mu\text{m/s}$ , respectively)]<sup>6,8</sup> in Fig. 2. Therefore, the adsorbed layer film is formed by two different molecular arrangements of surfactant molecules.

Control experiment curves were performed using  $\text{Si}_3\text{N}_4$  and platinum tips immersed in the Milli-Q Plus water mica double layer. One of the force versus separation control curves, performed using a  $\text{Si}_3\text{N}_4$  tip, is shown by the  $\bullet$  symbol in the inset of Fig. 2.

In Fig. 2, curves I and II show that in surfactant solutions the attractive and repulsive long-range components are displaced by the surfactant layer extend indicated by  $W_I$  and  $W_{II}$  when compared to the curve in water (inset,  $\bullet$ ). At  $(2.3 \pm 0.1)$  nm from the surface in region II [curves  $\triangle$  and  $\nabla$  in Figs. 2 and 3(a)], there is a rapid change in force with a small change in tip/surface separation. The value of the overall thickness of this layer is consistent with the formation of monolayers (the length of the fully extended molecule being about 2.2 nm). At sufficient large applied force ( $\sim 0.8$  nN)

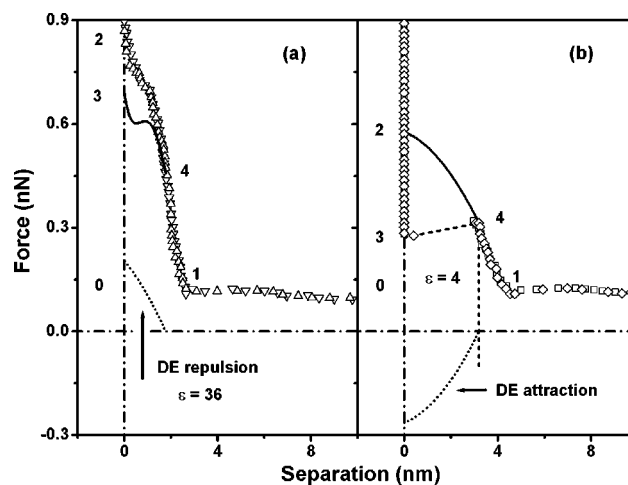


FIG. 3. Same as shown in Fig. 2. The dielectric exchange force acting on the tip when immersed in the surfactant layer, calculated for a tip with a spherical end with  $R \approx 5$  nm, indicated by the dotted line; (a) background region (curve II) and (b) islands (curve I). Point 1 corresponds to the compression force measured by the tip associated with the presence of the weakly adsorbed surfactant molecules in the tip/substrate interaction region.

the surfactant layer is removed from the space between the tip and the surface.

A different force curve is observed at region I [curves  $\square$  and  $\diamond$  in Figs. 2 and 3(b)]. The large repulsive deviation from the exponential component, starting at  $(4.4 \pm 0.1)$  nm from contact, is followed by an attractive regime, when the force achieves  $\sim 0.3$  nN, observed when the tip approaches the interface ( $\sim 3.2$  nm, which corresponds to the thickness of a bilayer). The attractive regime indicates that the layer compression is followed by an attraction of the tip by the layer present between the tip and substrate. Molecules forming thin layers should be easier to push away from the contact zone when compared to the ones forming thick layers, but the opposite is observed.

Let us now concentrate on the control experiment that was performed in pure water ( $\epsilon \approx 80$ ) in order to characterize the mica interface in the absence of adsorption layers (inset of Fig. 2,  $\bullet$ ). A simple analytical expression for the electrostatic force was previously derived<sup>9,10</sup> for a tip immersed in the mica double layer in water. The tip was defined to have a sharpened conical shape with a cone angle  $\alpha = 18^\circ$  and a flat end with radius  $R$  (microlever type-B Park tip). The displacement vector is assumed to have an exponential spatial dependence  $D(z) = D_0 \exp(-\kappa z/2)$ , where  $D_0$  is determined by the ionic charge distribution at the mica surface by using Gauss' Law. The elemental volume ( $dv$ ) of the tip immersed in the double-layer region is given by  $dv = \pi[R + (\tan \alpha)z]^2 dz$ , where  $z$  is the integration variable of the trapezoidal volume and  $H$  is the distance between the surface and the end of the tip. The change in the electric energy involved in the exchange of the dielectric permittivity of the double layer by that of the tip is calculated by integrating the energy expression over the tip-immersed volume in the double-layer region. The force is obtained by the gradient of the energy expression, i.e.,  $F_z = -\text{grad } \Delta E$ , where

$$\Delta E = \frac{1}{2\epsilon_0} \int_0^{10\kappa^{-1}-H} \left[ \frac{1}{\epsilon_{DL}(z)} - \frac{1}{\epsilon_{Tip}} \right] D^2(z) dv. \quad (1)$$

The force curves for water using  $\text{Si}_3\text{N}_4$  tips were matched by assuming a dielectric spatial variation [ $\epsilon_{\text{DL}}(H)$ ] at the interface, due to the effect of the mica interfacial charges on the orientation of the water molecules.<sup>9</sup>

The measured force versus separation curves for platinum-coated tips (not presented in this letter) show a different behavior when compared with those observed for  $\text{Si}_3\text{N}_4$  tips. This is the result of the fact that conductors have an infinite static permittivity, which corresponds to a null electric field inside the tip and, consequently, zero electric energy stored inside the tip volume. The corresponding force on the tip is then attractive since the immersion of the tip in the double-layer electric field minimizes the total energy of the configuration.

In order to explain the unexpected result that thin surfactant layers (background, region II) show higher rupture forces than thick layers (islands, region I), we propose that a distinct force component (attractive or repulsive) is present when the tip is immersed in thin or thick layers and its value is associated with its dielectric constant. To support our claims the force component when the tip is immersed in the surfactant layer was calculated using Eq. (1) assuming a half-spherical shape for the lower tip surface, since only its spherical part, with elemental volume  $dv = \pi[R^2 - (R - z)^2] dz$ , is immersed in the surfactant layers. The effect of the dielectric exchange force (DEF) when the tip is immersed in the region covered by a layer forming the background will be discussed first. The energy spent by approaching the tip to the interface corresponds to the area covered by the triangle (0-1-2) in Fig. 3(a); part of this energy will be fitted to the calculated energy associated with the force involved in the tip immersion in the surfactant layers with an adjustable value of dielectric permittivity. The result is shown by the dotted line in Fig. 3(a), indicated as ‘‘DE repulsion.’’ This energy component is subtracted from the experimental curve and the result is shown by the line 3-4. The value of  $\epsilon$  that best fitted this region is  $\epsilon \approx 36$ . This value is in agreement with the published ones for the dielectric permittivity of CTAB solutions at cmc.<sup>11</sup> The energy associated with the immersion of the tip in the thick layer is shown by the area [Fig. 3(b)], indicated by ‘‘DE attraction,’’ in the lower part of the force versus separation curve. If this component is subtracted from the original measured curve, we obtain a curve similar to the one measured when the tip is immersed in the thin layer, indicating that our fitting of the experimental curve is a reasonable calculated value of the attractive component. Consequently, the DEF gives a consistent description of the distinct force versus separation curves measured when the tip is immersed in a surfactant layer by assuming a thick layer with a dielectric permittivity  $\sim 4$  and a thin layer with  $\epsilon \approx 36$ .

As in previous studies, mica surfaces immersed in  $10^{-5}$  M CTAB concentration solutions were found not to be completely covered, lending support to the idea that absorption is in the form of aggregates.<sup>6</sup> These aggregates or islands have a 3.2 nm overall thickness and strongly resemble bilayer fragments, as previously reported.<sup>12</sup> The evidence for

bilayer formation presented in this work at region I is conclusive, since the measured thickness before rupture is 3.2 nm and the dielectric permittivity value of  $\epsilon \approx 4$  was measured. Thus, at region I the adsorbed layer film is formed by a highly compact molecular arrangement; these aggregates have fused sufficiently to form intercalated bilayer structures.

The measured value of the thin region (which corresponds to the monolayer) dielectric permittivity,  $\epsilon \approx 36$ , indicates that there is a significant fraction of water in the layers<sup>12</sup> associated with its high value of dielectric constant. Force versus separation curves are then particularly useful for discriminating between monolayer and bilayer formation, since both thickness and dielectric permittivity of the structure are simultaneously measured.

At sufficiently large applied force, the surfactant layer is squeezed from the space between the tip and the surface. This value is defined as the film rupture force and it is equal to  $\sim 0.8$  nN for the background region and  $\sim 0.3$  nN for the islands. Previous results identify this rupture force with steric limitations imposed by the immobilization of CTAB and by the location of the CTAB binding site at the mica surface.<sup>6</sup> The results shown in the previous paragraphs demonstrate that the DEF accounts for the difference in the rupture force of the two layers with different thicknesses and dielectric permittivities.

In summary, using AFM, we have investigated the adsorbate structure formed by a cationic surfactant (CTAB) on a hydrophilic surface (mica) in contact with an aqueous surfactant solution. The electrostatic force component associated with the immersion of the tip with  $\epsilon_T$  in a surfactant layer with  $\epsilon_S$  is a determining factor in the amplitude of its rupture force. The measured microscopic properties of the adsorbed layer may help to build a clear picture of the adsorbed CTAB molecular configuration on mica surfaces immersed in water.

The authors are grateful to J. R. Castro and L. O. Bonugli for technical assistance and acknowledge economical support from CNPq Grant No. 523.268/95-5 and FAPESP Grant No. 98/14769-2.

<sup>1</sup>J. P. Rabe, in *Nanostructures Based on Molecular Materials*, edited by W. Göpel and C. Ziegler (VCH, Weinheim, 1992).

<sup>2</sup>J. M. H. M. Scheutjens and G. J. Fleer, *J. Phys. Chem.* **84**, 178 (1980).

<sup>3</sup>P.-G. de Gennes and P. Pincus, *J. Phys. (France) Lett.* **44**, L241 (1983).

<sup>4</sup>L. Bergstrom and E. Bostedt, *Colloids Surf., A* **49**, 183 (1990).

<sup>5</sup>C. J. Drummond and T. J. Senden, *Colloids Surf., A* **87**, 217 (1994).

<sup>6</sup>O. Teschke, G. Ceotto, and E. F. de Souza, *J. Vac. Sci. Technol. B* **18**, 1144 (2000).

<sup>7</sup>W. A. Ducker, T. J. Senden, and R. A. Pashley, *Langmuir* **8**, 1831 (1992); H.-J. Butt, M. Jaszke, and W. A. Ducker, *Bioelectrochem. Bioenerg.* **38**, 191 (1995).

<sup>8</sup>M. W. Rutland and J. L. Parker, *Langmuir* **10**, 1110 (1994).

<sup>9</sup>O. Teschke, G. Ceotto, and E. F. de Souza, *Chem. Phys. Lett.* **326**, 328 (2000).

<sup>10</sup>O. Teschke and E. F. Souza, *Appl. Phys. Lett.* **74**, 1755 (1999).

<sup>11</sup>S. B. Johnson, C. J. Drummond, P. J. Scales, and S. Nishimura, *Langmuir* **11**, 2367 (1995).

<sup>12</sup>G. Fragneto, R. K. Thomas, A. R. Rennie, and J. Penfold, *Langmuir* **12**, 6036 (1996).